PETROPHYSICAL ROCK TYPING OF COQUINAS FROM THE MORRO DO CHAVES FORMATION, SERGIPE-ALAGOAS BASIN (NORTHEAST BRAZIL)

José Leão de Luna[1], Fabio Andre Perosi[1], Mariléa Gomes dos Santos Ribeiro[1], Andre Souza[3],
Austin Boyd[3], Leonardo Fonseca Borghi de Almeida[2] and Patrick William Michael Corbett[2,4]

ABSTRACT. This work has analyzed, considering the petrophysical point of view, samples of Coquinas obtained in the outcrop of the Morro do Chaves formation (Sergipe-Alagoas Basin). The complex sedimentological aspects for this study have been reduced by focusing on **a single bed**. The reservoirs found in this basin have the same age of the reservoirs of Campos, Santos and Espírito Santo Basins (Brazil) and Congo (Africa), from the end of Barremian to the beginning of Aptinian ages, which can be considered analogs of those ones. The data were collected applying routine core analysis and special core analysis techniques in five samples taken vertically, reproducing the case in a single well through a bed of coquinas, with a spacing of approximately 20 cm between each one, to replicate what might be sampled in subsurface coring operations. Measurements of porosity and effective permeability by gas expansion, Nuclear Magnetic Resonance and resistivity were conducted. The analysis of the data revealed the heterogeneity of the porous space in terms of pore sizes and correlations between permeability and electrical formation factor. Along with this detailed analysis, a petrotyping classification of the samples was done using the Global Hydraulic Elements method, to compare with a larger poro-perm data set from a lateral profile. This work shows that the heterogeneity in these few samples from a single bed along a vertical profile is representative for heterogeneity over a much larger coquina data set from the same bed away from this single profile. This work has implications for the scaling and interpretation of NMR data from plug data to log data in these sequences and the resulting prediction of permeability from the latter.

Keywords: carbonate, porosity and permeability properties, NMR, electrical resistivity.

RESUMO. Esse trabalho analisa, considerando o ponto de vista petrofísico, amostras de Coquinas obtidas em afloramento da Formação Morro do Chaves (Bacia de Sergipe–Alagoas). Os aspectos sedimentológicos complexos envolvidos neste estudo foram reduzidos, focando **em uma única camada**. Os reservatórios encontrados nesta bacia têm a mesma idade dos reservatórios das Bacias de Campos, Santos e Espírito Santo (Brasil) e Congo (África), final do Barremiano ao início do Aptiano, as quais podem ser consideradas análogas daquelas. Os dados foram obtidos por meio de técnicas de petrofísica básica e petrofísica especial em cinco amostras extraídas verticalmente, reproduzindo o caso de um único poço através de uma camada de coquinas, com um espaçamento de aproximadamente 20 cm entre cada uma, de forma a replicar o que poderia ser amostrado em uma operação de retirada de plugs em subsuperfície. Medidas de porosidade e permeabilidade efetiva por expansão de gás, Ressonância Magnética Nuclear e resistividade foram obtidas. A análise dos dados revelou a heterogeneidade do espaço poroso em termos de tamanho de poros e correlações entre permeabilidade e fator de formação elétrico. Junto a essa análise detalhada, foi realizada a classificação petrofísica das amostras pelo método de Elementos Hidráulicos Globais, para comparar com um conjunto maior de dados permo-porosos provenientes de um perfil lateral maior. Este trabalho mostra que a heterogeneidade nestas poucas amostras de uma única camada ao longo de um perfil vertical é representativa da heterogeneidade sobre um conjunto de dados de coquinas muito maior da mesma camada, afastados deste único perfil. Este trabalho tem implicações para a interpretação e escalonamento de dados de Ressonância Magnética Nuclear de plugues para dados de perfil de poço nesta sequência e para a predição da permeabilidade a partir destes.

Palavras-chave: carbonato, propriedades permoporosas, RMN, resistividade elétrica.

[1] Universidade Federal do Rio de Janeiro, IGEO – CCMN, LAGEP, Departamento de Geologia, Av. Athos da Silveira Ramos, 274, Sala J0-007, Cidade Universitária, 21941-916 Rio de Janeiro, RJ, Brazil. Phone: +55(21) 2590-8091 / Ramal 4 – E-mails: joselluna@gmail.com; faperosi@geologia.ufrj.br; marilea@geologia.ufrj.br

[2] Universidade Federal do Rio de Janeiro, IGEO – CCMN, LAGESED – Departamento de Geologia, Av. Athos da Silveira Ramos, 274, Sala J1-015/017, Cidade Universitária, 21941-916 Rio de Janeiro, RJ, Brazil. Phone: +55(21) 3938-9487 – E-mails: lborghi@geologia.ufrj.br; p.w.m.corbett@hw.ac.uk

[3] Schlumberger Brazil Research and Geoengineering Center, Rua Paulo Emídio Barbosa, 485, Quadra 7B, 21941-907 Rio de Janeiro, RJ, Brazil.
E-mails: ASouza19@slb.com; boyd2@slb.com

[4] Institute of Petroleum Engineering, School of Energy, Geoscience, Infrastructure and Society, Heriot-Watt University, Riccarton, Edinburgh, UK, EH14 4AS
– E-mail: p.w.m.corbett@hw.ac.uk

INTRODUCTION

Carbonate formations are responsible for about 50% of the petroliferous reservoirs around the world (Ramakrishnan et al., 2001). Many recent studies have been conducted to infer petrophysical properties of such reservoirs (examples include Al-Shahwan & Al-Iessa, 2015; Goda et al., 2007; Taktak et al., 2011; Ballay et al., 2007; Knackstedt et al., 2007; Sadeq & Yusoff, 2015; Eberli et al., 2003) aiming to understand and describe the behavior of those systems under oil production. Such reservoirs are strongly marked by heterogeneity in their porous space, which is strongly influenced by effects as dissolution, precipitation, re-precipitation, dolomitization and fracturing that, differently from siliciclastic reservoirs (e.g. sandstones), results in a space with pore dimensions composed by two or three distinct modes. As noted by Câmara (2013), most of these carbonate reservoirs, responsible for a large portion of world's hydrocarbon production, originated from carbonates deposited in marine environments. In Brazil, the study of lacustrine carbonate depositional environments, mainly the Coquinas, has a long history with the discovery of Pampo, Badejo, Linguado and Trilha reservoirs in Campos Basin during the 70's, and are described by several authors with respect to various sedimentological, stratigraphic and petrophysical properties (Feijó & Pereira, 1994; Azambuja & Arienti, 1998; Campos Neto et al., 2007; Câmara, 2013; Tavares et al., 2015).

With the discovery of additional high production capacity areas from lacustrine carbonates (microbialites and Coquinas) in the Pre-Salt interval of Santos Basin, the scenario has been changed, and more effort and investment in research are being done to characterize these rocks.

In comparative terms, Sergipe-Alagoas Basin, specifically the Morro do Chaves formation, presents a thick and extensive coquina sequence with many geological characteristics, very similar to the producing Coquinas of the Pre-Salt (Kinoshita, 2010). As a result the description and study of petrophysical parameters of these analogs at different scales can bring new and useful information for the characterization of Pre-Salt extracts. This represents a more detailed study at the bed scale to understand the heterogeneity present at that scale.

MATERIAL

The object of this study consists on a group of five plugs obtained from a layer of approximately one meter thick from an outcrop section of Morro do Chaves formation (Sergipe-Alagoas Basin). The measurements along a vertical profile were named as the 4A series (Fig. 1). Besides the data from these samples, porosity and permeability information were used from other series (horizontal profiles), for comparison. The 4A series is similar in appearance (Fig. 2) to other plugs from the same bed, presenting some amounts of visible moldic or vuggy porosities.

Figure 1 presents the sample's original layer, indicating the positions of the 4A series and the stratigraphic layer delimitation (Bed 2B layer), while Figure 2 shows the group of samples studied.

SAMPLE PREPARATION AND DATA ACQUISITION

In an experimental procedure, the samples were subject to cleaning by the Soxhlet method, i.e. a cycle of toluene to clean hydrocarbons and a cycle of methanol to clean salts. After that, they were dried in a moisture controlled oven (lab standard procedure), at 60°C for about 12 hours, and their weight measured until constant mass was observed. After that, porosity and permeability by Helium gas expansion method were measured with the application of 800 psi confining pressure, using a Coretest Systems Inc. (USA) AP-608 equipment.

To perform various laboratory measurements (NMR and electrical resistivity), the samples were fully saturated by applying isostatic pressure of 2,000 psi. The saturating fluid used was brine of 30,000 ppm NaCl concentration, with 1.043 g/cc density at 21.5°C (lab standard). Mass values of the samples were collected before and after saturation.

After saturation, the samples were wrapped in Teflon tape to minimize fluid evaporation during the experiments, and the NMR measurements carried out. Transversal relaxation time (T_2) was measured applying the CPMG pulse sequence (Coates et al., 1999), using a Maran Ultra DRX F (Oxford Inc., UK) equipment with resonance frequency of 2.6 MHz for the 1H nucleus. A total of 16,834 echoes were acquired and signal averaging performed to keep the signal-to-noise ratio always higher than 100. The main parameters of the NMR acquisitions are listed in Table 1.

Table 1 – Parameters applied to the NMR experiments.

Parameter	Value
Echo time	$400\mu s$
Number of averages	32
Waiting time between averages	10 s
90° pulse width	$12.2\mu s$
180° pulse width	$24.4\mu s$
Temperature	21°C

Electrical resistivity experiments were done using the Coretest Systems Inc. (USA) AERS-702 equipment that operates at room pressure and temperature of 22°C. The 2 terminal schedule, with

Figure 1 – Bed 2B layer, delimited by the white dashed lines, from where the 4A series were collected, vertically (series identified by the yellow arrow – about one meter thick). Further holes show plug locations that were not utilized for measurements in this study but have been used for poro-perm comparison (adapted from Corbett et al., 2016).

Figure 2 – 4A series studied. Naked eye analysis allows the observation of some vuggy or moldic porosity on the surface of the plugs.

30 psi connection pressure (electrode-sample), was used, applying an alternating current of 1 KHz frequency (lab standard). The brine resistivity was obtained through an immersion conductivity cell Orion (Thermo Electron Co., USA), resulting in the brine resistivity value of ρ_w = 0.128 ohm-m, at 21°C. After the measurements, the electrical resistance obtained was normalized to 20°C to standardize (R_t), given by equation (1):

$$R_t = R \left(\frac{T + 6.77}{Ts + 6.77} \right) \qquad (1)$$

where R is the measured resistance, T is sample's temperature during measurements and Ts is the temperature normalized to 20°C.

All data obtained was processed and analyzed to make possible the determination of the petrophysical parameters: effective porosity (gas, weight and NMR) and permeability, NMR T_2 relaxation time and pore size distributions, electrical formation factor (FF) and cementation exponent (m), which will be presented and discussed in the next section.

RESULTS AND DISCUSSION
Porosity, Pore Size Distribution and Partitioning
To determine porosity, techniques of NMR, Helium gas expansion and weight measurements were performed.

The porosity by weigh (ϕ_w) is obtained through the ratio between sample's mass before and after saturation process, together with brine's density, through equation (2):

$$\phi_w = \frac{\left(\frac{\text{saturated mass-dried mass}}{\text{brine density}} \right)}{\text{sample total volume}} \qquad (2)$$

The values of porosity obtained by the gas expansion (ϕ_G) and weight (ϕ_W) methods are showed in Table 2, together with the dried and saturated mass of the samples. To verify the quality of the saturation process, the saturation index (SI, in %) is calculated, given by the ratio between the weight to gas porosities. Gas expansion method is considered a more accurate result, since the application of the confining pressure assures that large pores located on the core's surface will be efficiently filled by the probing gas. The values of saturation index obtained are also showed in Table 2. Values between 98% and 102% are considered good.

Table 2 – Dried and saturated masses, porosity by weight and gas expansion methods, and saturation index (SI) calculated by the percentage between weight and gas porosity results.

Sample	Dried Mass (g)	Saturated Mass (g)	ϕ_W (%)	ϕ_G (%)	SI (%)
4.1A	127.315	134.573	12.6	13.6	92.9
4.2A	123.732	131.310	13.5	14.1	95.7
4.3A	131.067	140.354	15.3	15.7	97.7
4.4A	123.393	133.146	16.7	18.1	91.9
4.5A	138.461	144.960	10.6	11.8	90.2

Differences on saturation index of about 3-10% were found, which can be explained by the inability to maintain the external large pore structures filled by the saturating fluid during the weight measurements. This textural characteristic of the samples will influence directly the NMR porosities as well, since these measurements are taken immediately after the weighting process.

The NMR signal is proportional to the total amount of fluid inside the porous space, and so, to extract porosity from this technique, a calibration measurement is necessary on a brine sample with a well-known volume in order to be compared with sample's results. Knowing the mass of the calibration sample and its density, the NMR signal is linked to the volume of the filled porosity for each sample (Coates et al., 1999), whose results are showed in Table 3 together with ϕ_W and ϕ_G for comparison.

Table 3 – Porosity by NMR, weight and gas expansion methods.

Sample	ϕ_{NMR} (%)	ϕ_W (%)	ϕ_G (%)
4.1A	12.5	12.6	13.6
4.2A	13.7	13.5	14.1
4.3A	15.2	15.3	15.7
4.4A	16.4	16.7	18.1
4.5A	10.5	10.6	11.8

NMR and weight porosities presented an excellent agreement. However, both results show lower values when compared to the gas one. This can be explained by the saturation issue state above, i.e. the lack of saturation of the external macro and moldic/vuggy porosities.

Beyond porosity, the NMR technique allows the estimation of the pore size distribution of a porous media (Coates et al., 1999). The NMR CPMG experiment measures the magnetization decay related to the nuclei spins that are filling the porous space, characterized by a decaying time constant called the transverse relaxation time (T_2). For the analysis of sedimentary rocks measured at room temperature, the acquired signal is converted to the T_2 distribution via an Inverse Laplace Transformation

method. For details on the procedure and signal processing to obtain the distribution of T_2, see (Coates et al., 1999). In this application, each pore will generate a signal that decays with a single T_2 relaxation time, given by equation (3):

$$
\begin{aligned}
\frac{1}{T_2} &= \frac{1}{T_{2,Bulk}} + \frac{1}{T_{2,Surface}} \\
&= \frac{1}{T_{2,Bulk}} + \rho_2 \frac{S}{V}
\end{aligned}
\tag{3}
$$

where T_2 is the measured transversal relaxation time, $T_{2,Bulk}$ is the fluid's bulk relaxation time (in this case brine, equals to 2.7 s), $T_{2,Surface}$ is the relaxation time due to the rock/fluid interaction, S/V is the pore's surface area-to-volume ratio and ρ_2 is the surface relaxivity parameter, associated to the rock/fluid interaction. An additional relaxation phenomenon can play a role on T_2 relaxation rate of porous materials, the so-called diffusion term, which depends on rock's magnetic susceptibility, NMR experimental parameters (applied magnetic field strength and echo formation timing) and fluid's translational diffusion coefficient. However, for carbonates inside a low magnetic field as the one applied in this study, this term can be neglected and so the T_2 relaxation time distribution obtained can be interpreted as proportional to the sample's pore size distribution (since the presence of bulk relaxation will generate signals centered around a single value, the fluid's $T_{2,Bulk}$). Figure 3 shows the T_2 distribution for all the 4A series samples. The area under each distribution reflects the NMR porosity.

The distributions obtained span over 3 orders of magnitude, a broad range that reflects the complexity and heterogeneity of the Coquinas samples from this single bed. A small influence of $T_{2,Bulk}$ term is seeing (signals around 2 to 3 seconds), and so this relaxation rate can be neglected. This allows the interpretation of the obtained distributions as a reflection of core's pore size distribution, given by the $T_{2,Surface}$ term of equation (3).

To convert T_2 distributions to pore size distributions, as described by the surface term of equation (3), the surface relaxivity parameter (ρ_2, which characterizes the relaxation phenomenon due to the rock/fluid interaction) must be determined. This was done through the acquisition of the bi-dimensional Diffusion-T_2 map (not shown), whose experimental details are described in (Souza et al., 2013). Table 4 shows the obtained values.

Applying equation (3) and calculating S/V as a function of pore radius, the conversion of the T_2 distribution to pore radius distribution can be described by equation (4):

$$
r(T_2) = C \cdot \rho_2 \cdot T_2
\tag{4}
$$
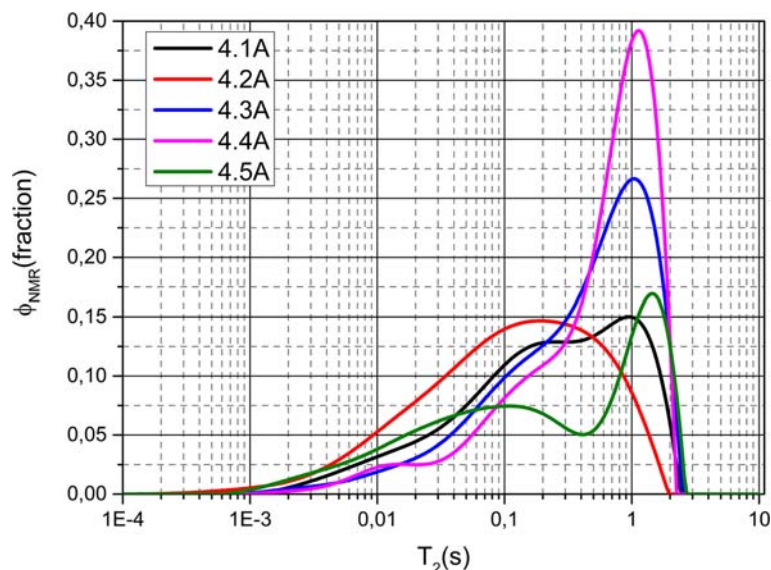
Figure 3 – Distribution of the transversal relaxation time, T_2, whose areas were normalized to match ϕ_{NMR}, for all samples.

where T_2 is the measured relaxation time, ρ_2 is the surface relaxivity and C is the geometrical factor that models the pores as spheres (3), cylinders (2) or parallel plates (1).

Table 4 – Surface relaxitivity parameters (ρ_2) obtained.

Sample	ρ_2 (μm/s)
4.1A	38.7
4.2A	37.1
4.3A	29.8
4.4A	33.5
4.5A	39.7

Using those ρ_2 values and $C = 3$, that considers the spherical geometry to the pores, the transversal relaxation time distributions of Figure 3 can be converted to pore sizes, making possible the partitioning of the distributions into micro, meso and macroporosities as used by Machado et al. (2011) and depicted in Figure 4.

Figure 5 shows the distributions of pore sizes for the samples, with the resulting porosity partitioning. At this point, it is clearly seen that even if one consider a larger T_2 range for the bulk relaxation influence (e.g. 1 to 3 seconds) (Machado et al., 2011), the resulting macroporosity fractions would not be affected since these signals are located far above the respective cutoff applied.

From pore size distributions shown in Figure 5 and the cutoffs assumed, the relative porosities for the adopted partitioning were calculated to quantify micro, meso and macroporosity fractions. Table 5 lists the findings, whose sum must be equal to total NMR porosity, and also the percentage of each partition relative to total ρ_{NMR}.

The proportions found clearly indicate that macroporosity is the predominant porosity fraction, responding in average for approximately 82% of total porosity, while mesoporosity responds to approximately 17%. Microporosity is very small, responding for approximately 2.2% of total porosity in average. Samples 4.3A and 4.4A presented the highest amount of macroporosity, together with the lowest amount of mesoporosity, 1.7 and 1.3%. Considering the relatively constant values found for their surface relaxivity parameter (see Table 4), one can affirm that the differences observed on the T_2 distributions would be mostly caused by differences related to the size of the pores.

**Electrical Resistivity, Formation Factor and Cementation Exponent**

The classical model of electrical resistivity (ρ_a) for homogenous samples will be considered here, expressed by equation (5):
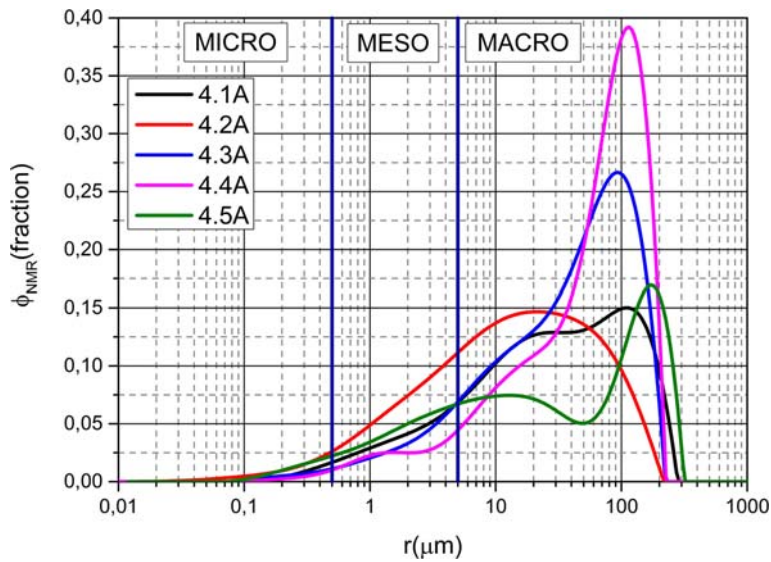
$$\rho_a = R\frac{A}{l} \qquad (5)$$

where R is the electrical resistance measured, A the area of the transversal section of the samples and l their lengths. Table 6 shows the ρ_a obtained.

As the brine resistivity (ρ_w) is known, the Formation Factor (FF) can be calculated through equation (6):

$$FF = \frac{\rho_a}{\rho_w} \qquad (6)$$
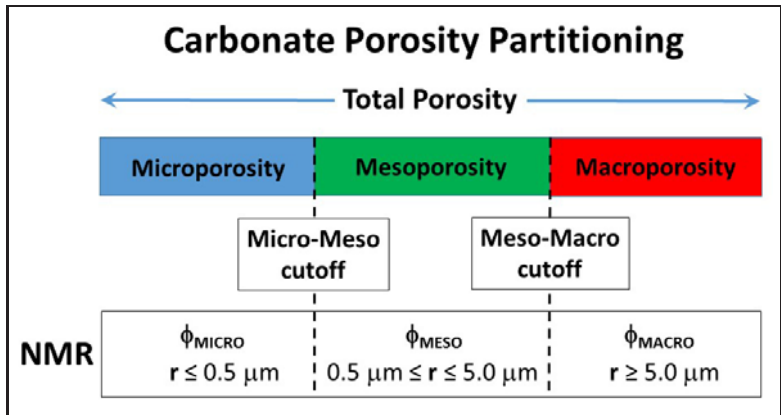
Figure 4 – Scheme of the carbonate porous space partitioning used, adapted from Machado et al. (2011).

Figure 5 – Pore size distributions obtained by NMR, with carbonate porosity partitioning proposed by Machado et al. (2011).

Table 5 – Porosity partitioning according to the classification by porosity type (micro, meso and macroporosity), and their percentage of total NMR porosity (ϕ_{NMR}).

Sample	Porosity Partitioning			% of total ρ_{NMR}		
	ρ_{MICRO} (%)	ρ_{MESO} (%)	ρ_{MACRO} (%)	MICRO	MESO	MACRO
4.1A	0.2	2.0	10.3	1.6	16.0	82.4
4.2A	0.5	3.4	9.8	3.7	24.8	71.5
4.3A	0.2	1.7	13.3	1.3	11.2	87.5
4.4A	0.1	1.3	15.0	0.6	7.9	91.5
4.5A	0.4	2.3	7.8	3.8	21.9	74.3

where ρ_a is the resistivity obtained through equation 5. The FF values found are also listed in Table 6.

Considering the Archie equation (Doveton, 2014), the Formation Factor (FF) can be expressed as a relation between porosity and cementation exponent (m) through equation (7):

$$FF = \frac{1}{\phi^m} \qquad (7)$$

The porosity used to calculate FF was the NMR derived one, since resistivity measurements were done without confining pressure. Thus, as observed for the NMR experiments, the external macropores were empty during acquisition of plug's resistances. Table 6 shows the FF obtained for the 4A series.

The so-called "generalized Archie equation" substitutes the unitary numerator in equation (7) by a parameter commonly called "electrical tortuosity" (Doveton, 2014). However, the original Archie formulation (given by Eq. (7)) is more appropriate for heterogeneous samples, like the Coquinas studied here, since it is not expected all samples to have the same electrical tortuosity. Data of NMR distributions shown in the previous section and Helium gas expansion permeability (presented and discussed in the next section) show high variability, confirming this assumption. An appropriate method to calculate this constant would be the determination of FF for several saturation states of a core. The estimation of a unique electrical tortuosity for a set of cores, however, can be done for a highly homogeneous, constant lithology formation.

The exponent m is often referred as a parameter that depends on the degree of the inter-particle porous space that are cemented, i.e. blocked by a substance, and so is a major obstacle to the electrical current's flow. Recent discussions are tending to redefine it, recognizing that a multiplicity of depositional and diagenetic process must play a crucial role on m (Doveton, 2014). For this reason, a modern and more accurate name for cementation coefficient is "porosity exponent". The m results found here for the 4A series will be interpreted based on this modern definition, where different and specific porosity types explain its variation.

Figure 6 shows a log-log plot of FF versus ϕ_{NMR}, following Archie's model of equation (7). The correlation reveals a fairly linear dependence, with a R^2 of 94.7%. Despite such good correlation, no numerical estimates were based on that fitting due to the heterogeneity of the samples and lack of knowledge about their tortuosities. The purpose of this plot is to show the strong dependence of FF with ϕ_{NMR}, revealing the importance of such analysis.

For each sample, m was calculated based on the log-log linearization of equation (7), given by equation (8):

$$m = -\frac{\log_{10} FF}{\log_{10} \phi_{NMR}} \qquad (8)$$

According to Schön (2004), Tiab & Donaldson (2012) and Doveton (2014), carbonates with m higher than 2 presents a significant amount of vuggy porosity, while values lower than 2 are presented by carbonates with predominance of inter-particle and fractured porosities. The term vuggy porosity is synonymous with macropore for the purpose of this study. Definition of inter-particle porosity for carbonates takes a very comprehensive meaning, aiming to consider several types of inter-crystalline and intergranular spaces (Doveton, 2014). Vuggy porosity incorporates large spaces mostly caused by particle and matrix dissolution, here it is often the shells alone that dissolve (i.e., moldic porosity), while fractured ones can be generated by other processes that are difficult to interpret based only on indirect exploratory methods (Doveton, 2014). Table 6 lists the m values extracted from the electrical resistivity measurements by equation (8).

Table 6 – Resistivity values (ρ_a), Formation Factor (FF) (considering the resistivity of $\rho_w = 0.128$ ohm-m for the bulk brine) and porosity coefficient (m), extracted from the electrical measurements.

Sample	ρ_a (ohm-m)	FF	m
4.1A	6.75	52.70	1.91
4.2A	6.19	48.32	1.95
4.3A	4.83	37.74	1.93
4.4A	4.91	38.36	2.02
4.5A	9.62	75.09	1.92

All the samples presented m values ranging between 1.91 and 2.02, which means that disconnected vuggy porosity should be very low with a predominance of inter-particle porosity. FF values were lowest for samples 4.3A and 4.4A, and increasing values were found for samples 4.2A, 4.1A and 4.5A, respectively. Also, FF data did not correlate well with m parameter, which can be explained as a consequence of a significant variation of porosity. ϕ_{NMR} have shown to vary between 10.5% and 15.2%, a difference of about 50% considering the lowest ϕ_{NMR} value of sample 4.5A. In conclusion, despite the high linearity seen on Figure 6, the derived m values have demonstrated to be a complex function of porosity fractions and types that characterize the studied samples.

Next sections will present and discuss permeability data that will lead, together with porosity results, to the development of a
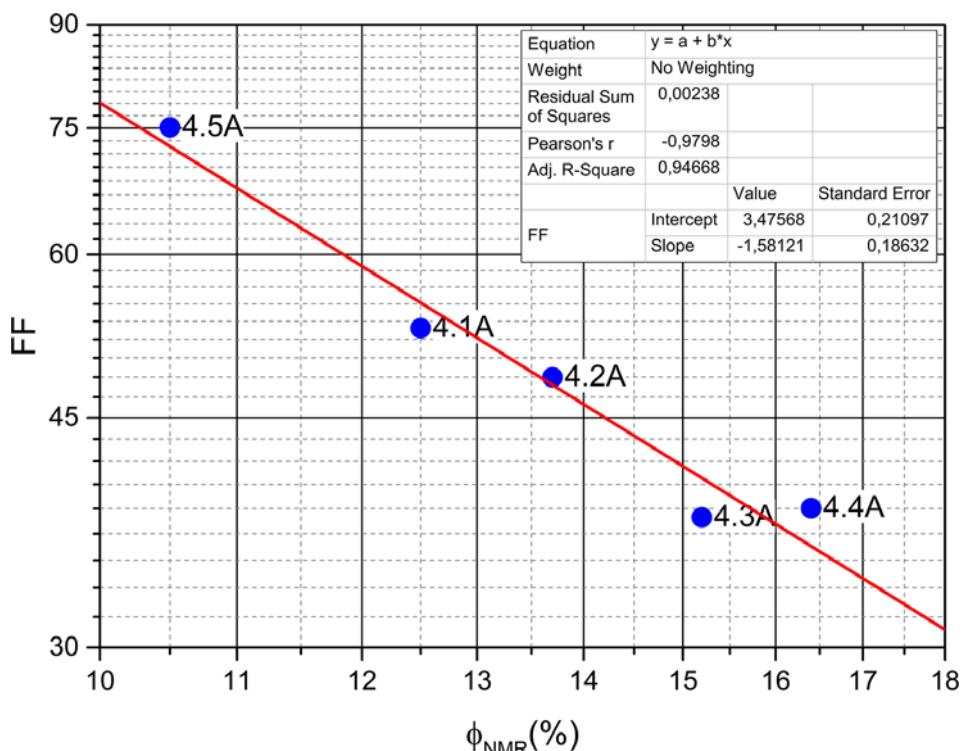
Figure 6 – Electrical formation factor (FF) versus ϕ_{NMR} correlation for the 4A series samples. The red solid line represents the fitting of the data, showing a very good linear correlation with a R^2 of 94.67%.

"petrotype" classification inspired by the work of Corbett & Potter (2004). This is a petrophysical rock typing method that will then be supported by the NMR and electrical resistivity findings.

Permeability and Global Hydraulic Elements Classification

Permeability (k) measures the flow capacity of a porous media related to a specific percolating fluid. Therefore, it is dependent on the porosity (primary and secondary), wettability, tortuosity and the connectivity of the pores, besides the environmental pressure conditions. Due to the high heterogeneity of Coquinas, one can observe a high variety in permeability of 4A series, ranging from about 20 to 600 mD. Table 7 presents the values of porosity and permeability obtained by the Helium gas expansion method.

Table 7 – Porosity (ϕ_G) and permeability (k_G) by gas expansion method.

Sample	ϕ_G (%)	k_G (mD)
4.1A	13.6	80.50
4.2A	14.1	20.62
4.3A	15.7	597.62
4.4A	18.1	393.75
4.5A	11.8	34.13

The understanding of the relations between porosity and permeability becomes necessary for the assessment of the system behavior as a possible reservoir. According to Akbas (2005), the correlation between permeability and porosity are usually linear models, expressed as equation (9):

$$\log_{10}(k) = a \cdot \log_{10}(\phi) + b \tag{9}$$

where a and b are constant. This analysis is generally called poro-perm correlation. Figure 7 shows the correlation plot of both properties, called the k-ϕ plot, where the model given by equation (9) were applied for the 4A series. The linear fitting applied have resulted in a fairly good adjustment, presenting a R^2 of 44.6%.

Considering the limited number of samples studied, data from 32 plugs extracted from the horizontally delimited Bed 2B layer (white dashed lines shown in Fig. 1) were studied, to check the k-ϕ properties along the formation. The obtained k-ϕ plot is shown in Figure 8, with the adjustment to the proposed linear model (red solid line) resulting in a R^2 of 72.9%. The equation and exponents that best adjusted the model were given by equation (10):

$$\log_{10}(k) = 8.29 \cdot \log_{10}(\phi) - 7.59 \tag{10}$$
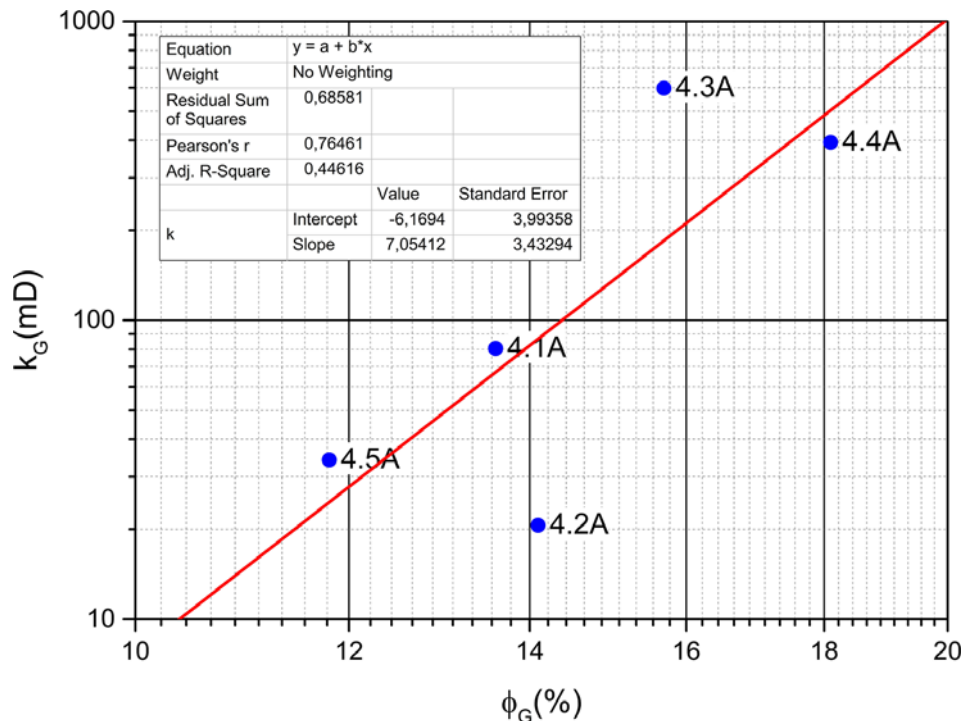
Figure 7 – k-ϕ plot of gas expansion method results, with linear fitting given by equation (9) (red solid line) for the poro-perm pairs of 4A series samples.
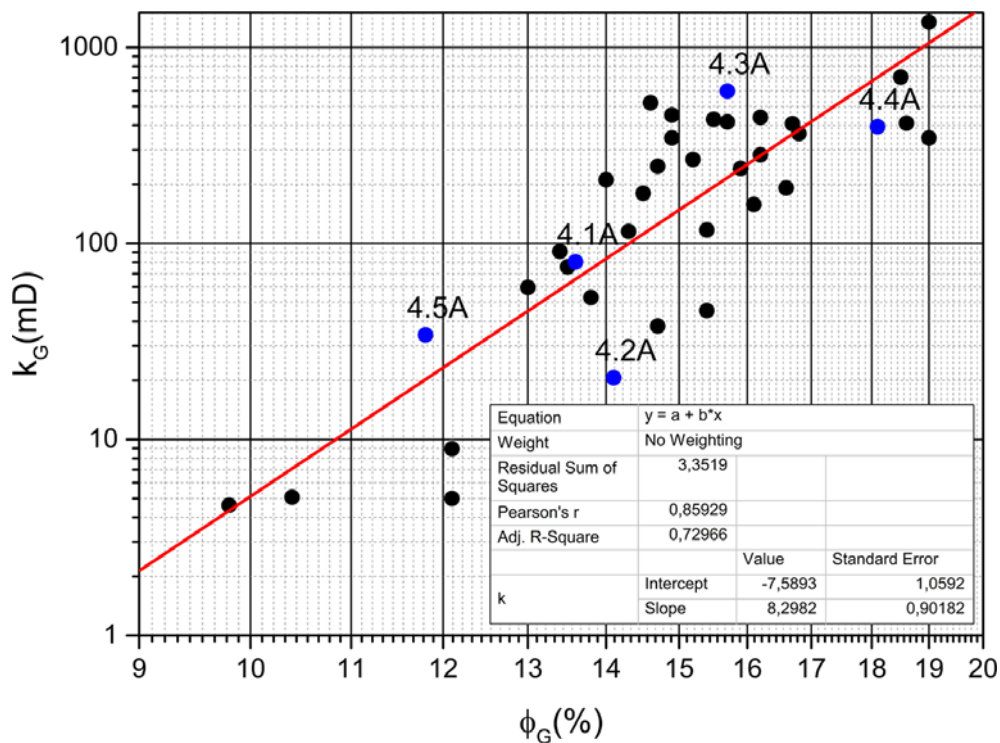
Figure 8 – k-ϕ plot with linear fitting for the poro-perm data considering all the samples obtained from the Morro do Chaves Formation: 4A series (blue circles) and horizontal Bed 2B layer (black circles). Note that the fit (red full line), whilst statistically reasonable, exhibits a significant variability not captured by the regression. Consequently, the resulting fitting will lead to poor permeability prediction if used for that purpose.

From the plot, it is clear that the 4A series samples are good representatives of the k-ϕ properties for the whole Bed 2B, no matter if horizontal or vertically sampled, justifying their choice for the detailed petrophysical analysis done.

Another important application of the poro-perm correlation is the classification of the system in terms of Hydraulic Units (HU), defined as a classification method that aggregates representative elementary volumes by similar poro-perm petrophysical and geological properties of a reservoir (Câmara, 2013). The obtained HU must be internally consistent and sufficiently distinct from other units that affects the hydraulic flow of such formation (Câmara, 2013). These units are obtained through the porosity and permeability analysis, generating groups by the calculation of the Flow Zone Index (FZI) parameter, expressed by equation (11):

$$ FZI = \frac{0.0314\sqrt{\frac{k}{\phi}}}{\left(\frac{\phi}{1-\phi}\right)} \qquad (11)$$

Defining constant FZI zones, it is possible to locate the k-ϕ pairs inside different zones, allowing the classification of the samples in terms of consistent Global Hydraulic Elements (GHE) (Corbett & Potter, 2004). The resulting GHE zones and sample's classification are presented in Figure 9.

The advantage on the GHE classification is that it allows the identification of trends on the k-ϕ properties, through the regular progression of FZI (Corbett & Potter, 2004), and also a fairer comparison among samples of different origins.

The results show the presence of 3 GHE's (5, 6 and 7) with different hydraulic flow behaviors in the vertically sampled 4A series. The 32 k-ϕ pairs of the whole Bed 2B were also applied to the GHE classification, whose results are shown in Figure 10.

It is remarkable the fact that for all the samples, as shown by Figure 10, the same 3 distinct GHE's (5, 6 and 7) were found; those are exactly the ones found for the vertical 4A series. This fact encourages the correlations and discussions about the 4A samples, even considering it as a limited sample space case. It suggests that samples along a vertical profile (as the ones extracted by subsurface coring operations) can be extended laterally into the reservoir.

Petrophysical Rock Typing by GHE and Data Correlation
To facilitate the correlation of the acquired and discussed data, Table 8 presents a chart that resumes the key results obtained for the 4A series.

Considering the NMR pore size partitioning, FF results seem to be dependent on porosity, since the lower the FF, the higher the ϕ_{MACRO} and lower the ϕ_{MESO}. ϕ_{MICRO} values found were too small, and for this reason they will not be interpreted here. Sample 4.5A presented the highest FF and the lowest amount of macroporosity, although the expected trend was not observed for its mesoporosity fraction. Samples 4.1A and 4.2A presented similar FF and ϕ_{MACRO} values, but different ϕ_{MESO}. It is a fact that mesoporosity will influence the electrical current pathway, but in a complex manner, hard to unveil only with the acquired data. These correlations are important to be stressed, since they are not straightforward conclusions in complex systems as the Coquinas studied here.

Table 8 – Porosity (ϕ_G) and permeability (k_G) by gas expansion method.

	Sample				
	4.1A	4.2A	4.3A	4.4A	4.5A
ϕ_G (%)	13.6	14.1	15.7	18.1	11.8
ϕ_{NMR} (%)	12.5	13.7	15.2	16.4	10.5
ϕ_{MICRO} (%)	0.2	0.5	0.2	0.1	0.4
ϕ_{MESO} (%)	2.0	3.4	1.7	1.3	2.3
ϕ_{MACRO} (%)	10.3	9.8	13.3	15.0	7.8
k_G (mD)	80.50	20.62	597.62	393.75	34.13
FF	52.70	48.32	37.74	38.36	75.09
m	1.91	1.95	1.93	2.02	1.92
GHE	GHE6	GHE5	GHE7	GHE7	GHE6

It was surprisingly noted that m does not look to correlate well with FF and also with the NMR porosity partitioning proposed. According to Doveton (2014), the electrical properties of carbonates must depend on porosity differently from what is commonly seen in sandstones, in a way that not all the porosity fractions play a significant role in electrical conductivity through a complex carbonate rock sample. As m takes into account the total porosity, its value can be inaccurate and so FF looks to correlate better with NMR porosities and GHE zones. It is possible that the macropores are relatively uniformly distributed through these samples, hence the 'interparticle' m exponents. These macropores are therefore not connected vugs in the petrophysical sense.

Permeability data were grouped by the GHE method applied. Samples 4.3A and 4.4A, the most permeable ones, were grouped as GHE7. This element have shown to represent the best quality reservoir among the samples. This is corroborated by the good porosities (15% and 18%, approximately) found for this element, and permeabilities of approximately 600 and 400 mD. Samples 4.1A and 4.5A were grouped as GHE6, presenting porosities of approximately 14% and 12%, and permeabilities around 80 and 34 mD, respectively. Sample 4.1A was classified as belonging to GHE5, presenting the lowest permeability (20 mD) and an approximate porosity of 14%.
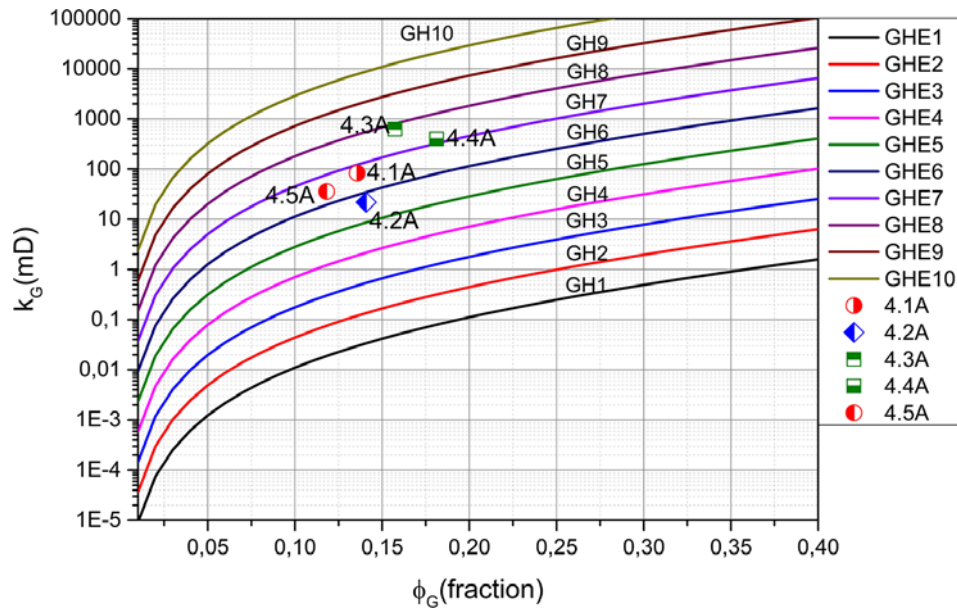
Figure 9 – GHE classification of the 4A series samples based on the porosity and permeability data. The limits of the GHE's are defined by the FZI parameter.
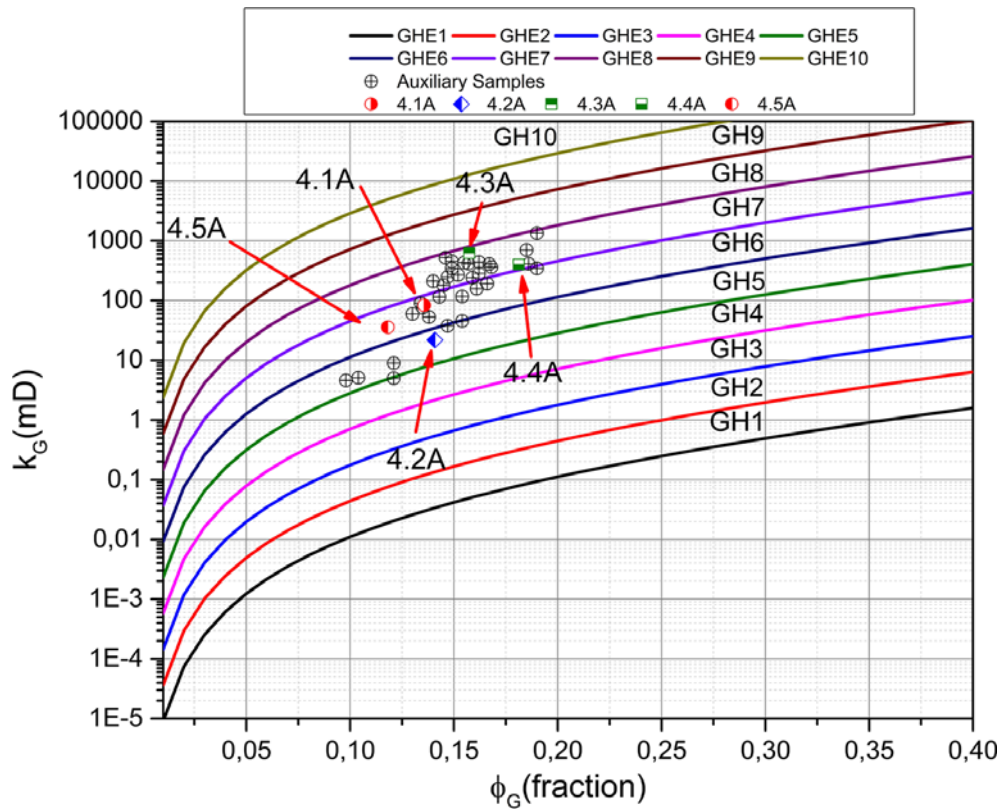

Figure 10 – GHE classification of the 4A series and the 32 Coquinas samples from the whole Bed 2B horizontal layer, based on the porosity and permeability data. The limits of the GHE's are defined by the FZI parameter.

As already described, FF was able to correlate with porosity, but m does not. At the same time, NMR ϕ_{MESO} porosity also correlated very well with permeability and FF (higher for the lowest permeable core – sample 4.2A, and lower for the highest ones – samples 4.3A and 4.4A). Meanwhile, the ϕ_{MACRO} porosity fails in predicting permeability, which can be understood in terms of the well-established concept that permeability is a property of pore throats, or the constrictions to the fluid's flow, most likely represented by ϕ_{MESO}.

With these conclusions in mind, it is feasible the proposition of a "petrotype" classification (an alternative name for the idea of petrophysical rock typing) (Corbett & Potter, 2014), that is able to predict petrophysical features of Coquinas base on the k-ϕ plots associated with the GHE zones. It was shown that the findings are strongly dependent on the amount of mesoporosity, defined as pores with sizes between 0.5 and 5.0μm. Macroporosity, defined as pores with sizes longer than 5μm, can play a role on the electrical resistivity properties, but a less important role on fluid transport properties. Microporosity, as defined, is very low in quantity, and so does not play an important role on permeability for these samples.

As a main conclusion of this work, NMR and electrical resistivity were able to support the GHE zones found that were, in turn, able to predict poro-perm properties. Moreover, the prediction of the petrophysical properties studied were proposed with a minimum of time (in data acquisition) and data availability.

To further corroborate and to provide a deep understanding of those findings, it would be necessary the acquisition of more data, able to elucidate key properties of Coquinas' geological aspects, like thin section and micro-computed Tomography (μ-CT) images (Corbett et al., 2017). Further correlation of those data will enlighten the role of important characteristics as cementation degree, pore types, sizes and their associated aspect ratios, and grain conservation. Besides, effects from physical-chemical processes that happened during their lithification processes will be very valuable to the consolidation of the discussions and conclusions made.

CONCLUSIONS

The Coquinas carbonate samples studied, extracted from a vertical profile in a single bed of the Morro do Chaves Formation, were characterized by a high degree of heterogeneity in their spatial petrophysical properties, especially regarding to their characteristic porous space. The significant presence of mesoporosity and a predominance of macroporosity were found by an adapted NMR pore size distribution partitioning method. A consequence of this fact is reflected in the cementation coefficient, which were observed to lie between 1.91 to 2.02, the lower limit of carbonates with high amounts of vuggy porosity. Electrical resistivity formation factor parameter shows a strong dependence with the macro-porosity fraction and a small effect on the poro-perm properties of the studied Coquina samples.

A "petrotype" classification was proposed, that uses the Global Hydraulic Elements method based on the k-ϕ plot. Three distinct GHE elements were successfully observed, corroborated by additional 32 samples extracted from the same formation along a horizontal profile. The resulting petrotyping definition revealed that all the samples have the same pore space characteristics: strong predominance of macroporosity, always higher than 70% of total porosity, medium mesoporosity fraction (about 16% of total porosity) and very low microporosity fractions (about 2-3% of the total porosity); and that even considering the high amounts of macroporosities found, the mesoporosity fractions were more successful in prediction the GHE zones and associated permeabilities.

The presented results and their inter-correlations will be further studied and refined in ongoing studies, with the addition of more petrophysical data from samples of the same formation, and also a comprehensive analysis of their geological characteristics.

REFERENCES

AKBAS CY. 2005. Determination of Flow Units for Carbonate Reservoirs by Petrophysical Based Methods. The Graduate School of Natural and Applied Sciences of Middle East Technical University. Degree of Master of Science in Petroleum and Natural Gas Engineering, August 2005, 148 pp.

AL-SHAHWAN MF & AL-IESSA IAA. 2015. Reservoir in Ratawi Oil Field, South of Iraq. Journal of Basrah Researches, 40: 44 A.

AZAMBUJA NC & ARIENTI LM. 1998. Guidebook to the Rift-Drift Sergipe-Alagoas, Passive Margin Basin, Brazil. The 1998 American Association of Petroleum Geologists International Conference and Exhibition.

BALLAY RE, MATHURIN G & PIASENTIN A. 2007. Petrophysical Characterization of Carbonate Formations for Geothermal Reservoir Analysis. Proceedings European Geothermal Congress, Unterhaching, Germany, 30 May-1 June.

CÂMARA RN. 2013. Caracterização petrofísica de coquinas da formação Morro do Chaves (barremiano/aptiano), intervalo pré-sal da bacia de Sergipe-Alagoas. Postgraduate Program in Geologia, Instituto de Geociências, Universidade Federal do Rio de Janeiro, Brazil, Unpubl. Master Dissertation, 112 pp.

CAMPOS NETO OPA, LIMA WS & CRUZ FEG. 2007. Bacia de Sergipe-Alagoas. Boletim de Geociências Petrobras, 15(2): 405–415.

COATES GR, XIAO L & PRAMMER MG. 1999. NMR Logging: Principles and Applications. Halliburton Energy Services, Houston, 234 pp.

CORBETT PWM & POTTER D. 2004. Petrotyping: a basemap and atlas for navigating through permeability and porosity data for reservoir comparison and permeability prediction. SCA Annual Conference, Abu Dhabi, UAE.

CORBETT PWM, ESTRELLA R, SHOIER A, MORALES A & BORGHI L. 2016. Integration of Cretaceous Morro do Chaves rock properties (NE Brazil) with the Holocene Hamelin Coquina architecture (Shark Bay, Western Australia) to model effective permeability, Petroleum Geoscience, 22: 105–122.

CORBETT PWM, WANG H, CÂMARA R, BORGHI L, MACHADO A, TAVARES A-C & BAGUEIRA R. 2017. Using the Porosity Exponent (m) and Pore-Scale Resistivity Modelling to Understand Pore Fabric Types in Coquinas (Barremian-Aptian) of the Morro do Chaves Formation, NE Brazil, submitted to Marine and Petroleum Geology.

DOVETON JH. 2014. Principles of Mathematical Petrophysics. Oxford University Press, 248 pp.

EBERLI GP, BAECHLE GT, ANSELMETTI FS & INCZE ML. 2003. Factors Controlling Elastic Properties in Carbonate Sediments and Rocks. The Leading Edge, 22(7): 654–660.

FEIJÓ FJ & PEREIRA MJ. 1994. Bacia de Sergipe-Alagoas. Boletim de Geociências da Petrobras, 8(1): 149–161.

GODA HM, BEHRENBRUCH P & MAIER HR. 2007. Alternative modelling approaches for the estimation of irreducible water saturation:

Australian hydrocarbon basins. Journal of Petroleum Science and Engineering, 57: 60–69.

KINOSHITA EK. 2010. Modelagem sismica-geometrica de facies dos carbonatos lacustres do Membro Morro do Chaves, Bacia de Sergipe-Alagoas, B. Geosci. Petrobras, 18(2): 249–269.

KNACKSTEDT MA, ARNS CH, SHEPPARD AP, SENDEN TJ, SOK RM, CINAR Y, OLAFUYI AO, PINCZEWSKI WV, PADHY G & LOANNIDIS M. 2007. Pore Scale Analysis of Electrical Resistivity in Complex Core Material. International Symposium of the Society of Core Analysts, Calgary, Canada, September 10-12.

MACHADO V, FREDERICO P, NETTO P, BAGUEIRA R, BOYD A, SOUZA A, ZIELINSKI L & JUNK E. 2011. Carbonate Petrophysics in Wells Drilled with Oil-Base Mud. SPWLA 52nd Annual Logging Symposium, Colorado Spring, May 14-18.

RAMAKRISHNAN TS, RAMAMOORTHY R, FORDHAM E, SCHWARTZ L, HERRON M, SAITO N & RABAUTE A. 2001. A Model-Based Interpretation Methodology for Evaluating Carbonate Reservoirs. The Society of Petroleum Engineers Annual Technical Conference and Exhibition, New Orleans, Louisiana.

SADEQ QM & YUSOFF WIWBW. 2015. Carbonate Reservoirs Petrophysical Analysis of Bai Hassan Oil Field North of Iraq. J. Bioremed. Biodeg., 6: 311.

SCHÖN JH. 2004. Physical Properties of Rocks, Fundamental and Principles of Petrophysics. Oxford: Elsevier Science Ltd., 583 pp.

SOUZA A, CARNEIRO G, ZIELINSKI L, POLINSKI R, SCHWARTZ L, HÜRLIMANN MD, BOYD A, RIOS EH, SANTOS BCC, TREVIZAN WA, MACHADO VF & AZEREDO RBV. 2013. Permeability Prediction Improvement using 2D NMR Diffusion-T_2 Maps. SPWLA 54th Annual Logging Symposium, New Orleans, Louisiana, June 22-26.

TAKTAK F, RIGANE A, BOUFARES T, KHARBACHI S & BOUAZIZ S. 2011. Modelling approaches for the estimation of irreducible water saturation and heterogeneities of the commercial Ashtart reservoir from the Gulf of Gabès, Tunisia. Journal of Petroleum Science and Engineering, 78: 376–383.

TAVARES AC, BORGHI L, CORBETT P, LOPES JN & CÂMARA R. 2015. Facies and depositional environments for the coquinas of the Morro do Chaves Formation, Sergipe-Alagoas Basin, defined by taphonomic and compositional criteria. Brazilian Journal of Geology, 45(3): 415–429.

TIAB D & DONALDSON EC. 2012. Petrophysics – Theory and Practice of Measuring Reservoir Rock and Fluids Transport Properties. 3rd ed.. Elsevier, 976 pp.

NOTES ABOUT THE AUTHORS

José Leão de Luna is a doctoral student in Geology (LAGEP/ IGEO/ UFRJ). It holds a BA in Physics (UFRJ, 2009) and Master in Geology (with emphasis on well logging – UFRJ, 2012). Served as a substitute professor (IGEO/ UFRJ). Main areas of interest are geophysical well logging and petrophysical, where assisted in several projects (acquisition and processing of well log data).

Fabio Andre Perosi is Associate Professor of Geophysics at undergraduate and graduate degrees in the Department of Geology, working in the LAGEP (Laboratory of Geophysics and Petrophysics) at Universidade Federal do Rio de Janeiro (UFRJ). Main research interests are Seismic and Gravimetric Methods, Well Logging and Petrophysics. Undergraduate in Physics (1997) from Universidade Federal do Rio Grande do Sul (UFRGS), M.Sc. (2000) and Ph.D. (2006) in Geophysics from Universidade de São Paulo (USP) and did a long-term internship (dec/2003-jul/2004) at U.S. Geological Survey, in Menlo Park, CA. Also has an interest in Geosciences and Physics Education.

Mariléa Gomes dos Santos Ribeiro received a B.Sc. in Electrical Engineering from Universidade Santa Úrsula (1995), a M.Sc. (2007) and a D.Sc. (2013) in Reservoir Engineering and Exploration from Universidade Estadual do Norte Fluminense. Specialist in well logging and petrophysical, presently is visiting researcher and professor of Geophysics Laboratory at Universidade Federal do Rio de Janeiro (UFRJ), Brazil.

Andre Souza is a Senior Research Associate at Schlumberger Brazil Research and Geoengineering Center, Rio de Janeiro, Brazil. M.Sc. and a Ph.D. in Material Science and Engineering from Universidade de São Paulo, Brazil, and a B.Sc. in Engineering Physics from Universidade Federal de São Carlos, Brazil. Joined Schlumberger in 2010 as an intern at Schlumberger-Doll Research in Cambridge, Massachusetts, USA. Main research interests are nuclear magnetic resonance applied to porous media characterization, petrophysics and geophysics.

Austin Boyd is the Managing Director at the Brazil Research and Geoengineering Center, in Rio de Janeiro. Prior to moving to Brazil, was Program Manager for Petrophysics at Schlumberger Doll Research. Before moving to research, held a variety of positions in interpretation development in the US and the Middle East. Joined Schlumberger in 1981 as a field engineer after receiving a B.Sc. in Electrical Engineering from Dalhousie University.

Leonardo Fonseca Borghi de Almeida Graduate (1989), Master (1993) and Ph.D. (2002) in Geology from the Universidade Federal do Rio de Janeiro. Currently, is Assistant Professor at UFRJ, where teaches, guides (undergraduate and graduate) and carries out research in several areas of Sedimentary Geology, in addition to coordinating the Sedimentary Geology Laboratory (Lagesed).

Patrick William Michael Corbett Graduated with a degrees in Geology (Exeter University, B.Sc. 1977), Micropalaeontology (University College London, M.Sc., 1978), Geological Statistics (Kingston University, PGDip, 1982), Petroleum Engineering (Heriot-Watt University, Ph.D., 1993) and Petroleum Geoengineering (Heriot-Watt University, D.Sc., 2006). Currently, is BG Group International Professor Colaborador Voluntário in Petroleum Geoengineering at UFRJ and has taught a Carbonate Petrophysics at a number of Brazilian Universities and elsewhere.